A&A 408, 187–192 (2003)
DOI: 10.1051/0004-6361:20030853

Astronomy & Astrophysics

G107.5−1.5, a new SNR discovered through its highly polarized radio emission

R. Kothes⋆

National Research Council of Canada, Herzberg Institute of Astrophysics, Dominion Radio Astrophysical Observatory, PO Box 248, Penticton, British Columbia, V2A 6J9, Canada
Department of Physics and Astronomy, The University of Calgary, 2500 University Dr. NW, Calgary, AB, T2N 1N4 Canada

Received 12 March 2003 / Accepted 4 June 2003

Abstract. A new highly polarized shell-type supernova remnant (SNR) has been discovered in the Canadian Galactic Plane Survey (CGPS). The only part of the remnant visible in radio continuum is a thin shell segment sitting on top of diffuse emission. The curvature of this segment indicates a much larger object which is not detectable in our observations most likely due to an imhomogenous ambient medium. A comparison of 408 MHz and 1420 MHz continuum emission reveals a spectral index of $\alpha = -0.6 \pm 0.1$ ($S \sim \nu^{\alpha}$), typical for a shell-type SNR. The polarized intensity averaged over the object is 50% of the total intensity, and the peak fractional polarization is close to the theoretical maximum, making this remnant the most highly polarized SNR known. At the projected centre of the radio shell is the unidentified X-ray point source 1RXS J225203.8+574249 which could be the neutron star left behind by the supernova explosion or its pulsar wind nebula. From the low rotation measure and possibly related H I features a distance of about 1.1 kpc is proposed. At this distance the radius of G107.5−1.5 is about 6 pc. The morphology and the structure of the ambient neutral hydrogen around the SNR suggests that this supernova remnant is in a late stage of evolution.

Key words. ISM: individual objects: G107.5−1.5 – ISM: supernova remnants – magnetic fields – polarization

1. Introduction

Currently 231 supernova remnants have been identified in the radio band after decades of intensive search with the largest single antenna and synthesis telescopes (Green 2001). However, these observations are strongly biased, mainly by three selection criteria: a) the surface brightness of the SNR must be above the detection thresh hold of the observations, b) the remnant must be resolved by the observations otherwise it could be mistaken for an extra galactic source, and c) it must not be confused by surrounding thermal emission which could artificially increase the detection limit. On the other hand we know that the population of SNRs should be dominated by objects with low radio surface brightness. 80 to 90% of supernova explosions in Galaxies like ours are of type II or Ib/c (van den Bergh & McClure 1994). These are the explosions of massive progenitor stars many of which will have created stellar wind bubbles around them. An explosion in this environment can be expected to lead to an SNR with very low radio surface brightness because of the low ambient density within the bubble. We can also anticipate the presence of confusing thermal emission from gas ionized by other stars in the vicinity which have not yet exploded. The discovery of these faint objects requires a survey which combines high sensitivity with excellent angular resolution at low radio frequencies, to give high sensitivity to faint, filamentary, non-thermal emission. The Canadian Galactic Plane Survey (CGPS) meets these requirements as has already been demonstrated by the recent discovery of two faint supernova remnants which are confused by thermal emission (Kothes et al. 2001).

In this work I present the discovery of a faint supernova remnant which is the most highly polarized supernova remnant known.

2. Observations

The radio continuum and H I line data were obtained using the synthesis telescope of the Dominion Radio Astrophysical Observatory (Landecker et al. 2000) as part of the CGPS (Taylor et al. 2003). Single antenna data are incorporated into the synthesis maps to ensure accurate representation of all structures up to the largest scales. The low spatial frequency H I data are from the Low Resolution DRAO Survey of the CGPS region observed with the DRAO 26-m telescope (Higgs & Tapping 2000). Continuum data are derived from the 408-MHz All-Sky survey (Haslam et al. 1982), and from the 1.4 GHz Effelsberg survey (Reich et al. 1997). The angular resolution of the data varies slightly across the final maps as cosec(δ)(1420/ν(MHz)). At the position of the radio shell the resolution is 69″×59″ for the H I data, 57″×49″ at 1420 MHz,

⋆ e-mail: roland.kothes@nrc-cnrc.gc.ca

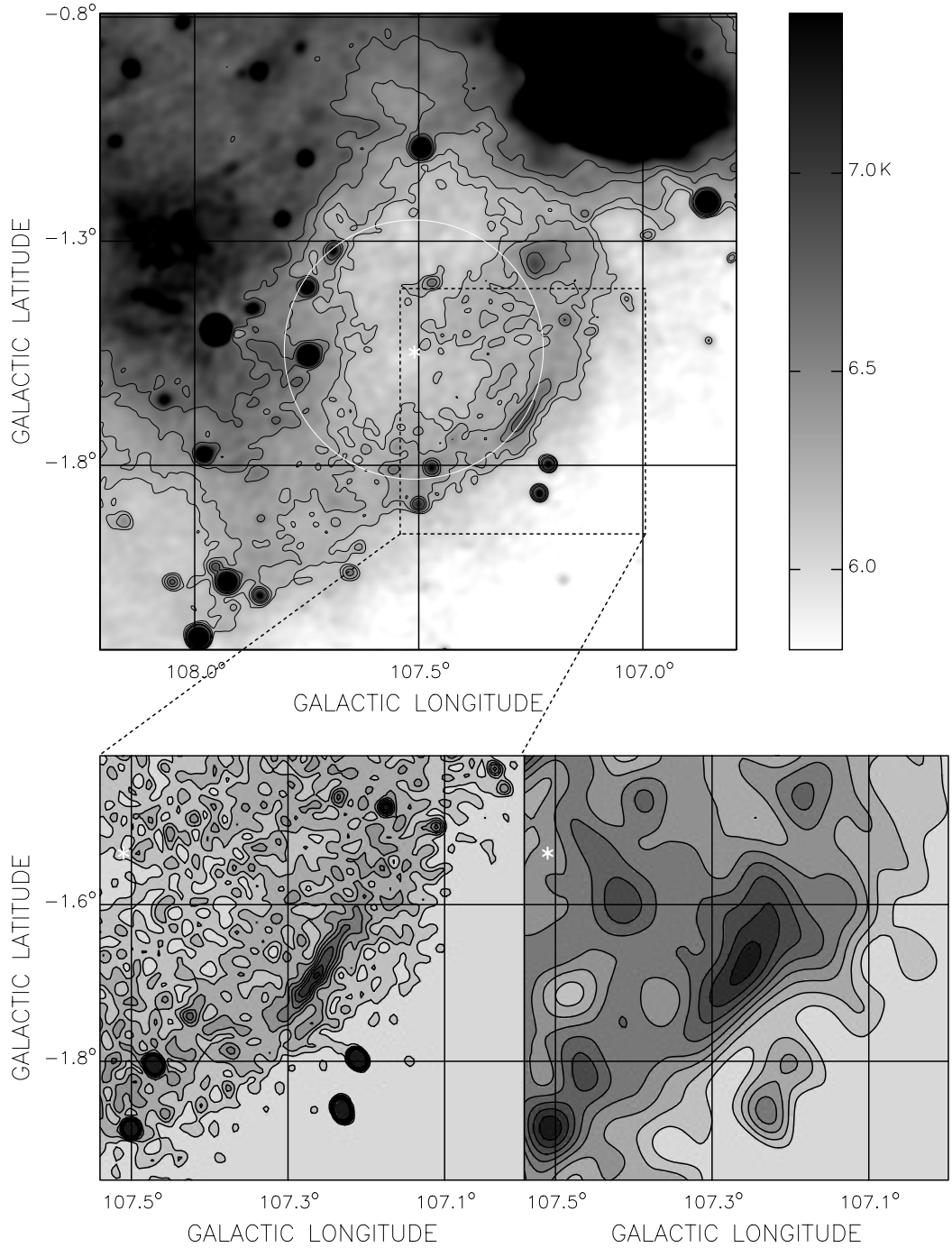

Fig. 1. Greyscale images of the new SNR G107.5−1.5 taken from the CGPS. In the upper panel a bigger area is displayed at 1420 MHz to locate the new SNR within its environment. The white star marks the position of the unidentified X-ray source 1RXS J225203.8+574249. The lower images are zoomed in on the radio shell as indicated at 1420 MHz (*left panel*) and 408 MHz (*right panel*). Contour levels are from 6.1 K to 7.15 K in steps of 0.15 K at 1420 MHz and from 63 K to 77 K in steps of 2 K at 408 MHz.

and $3\farcm5 \times 3'$ at 408 MHz at an angle of -62° (clockwise from north).

3. Results

3.1. Radio continuum emission

The new supernova remnant is located about 4° west of the extremely bright SNR Cas A in a rather complex area which is confused by diffuse background emission and several radio-bright H II regions (see Fig. 1). The brightest and largest of those is Sh 142, which is visible in Fig. 1 in the north-west corner of the upper panel. The general structure of this newly discovered SNR is most clearly seen at 1420 MHz (Fig. 1). The source appears as a thin filament on top of diffuse shell-like emission. The area the shock wave supposedly came from – deduced from the curvature of the filament – shows a void in the diffuse 1420 MHz continuum emission. The identification

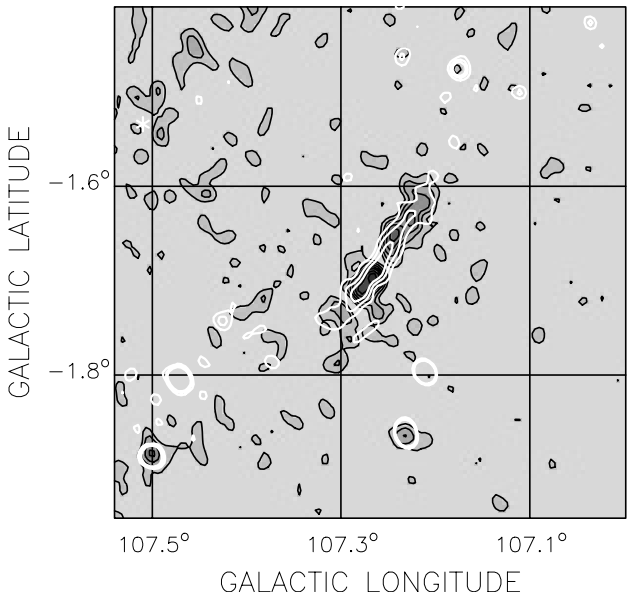

Fig. 2. Greyscale image of the new SNR G107.5−1.5 at 1420 MHz in polarized intensity taken from the CGPS. Contour levels are from 150 mK to 675 mK in steps of 75 mK. White contours indicate the total power emission. The position of the unidentified X-ray source 1RXS J225203.8+574249 is marked by a white asterisk.

as an SNR was mainly based on the highly polarized emission which is confined to the thin filament (Fig. 2). The structure and curvature of this shell segment suggests that it is part of a much larger remnant. The other parts of the SNR must be either in a much earlier stage of evolution, still expanding freely within material of very low density or in a much later stage already decelerated in material of very high density. In the first case the remnant would be larger than indicated by the curvature of the visible shell segment because the invisible parts would not be as much decelerated as the visible part. In the latter case the remnant would be smaller than indicated by the curvature of the visible shell segment because the invisible parts would be more decelerated than the visible part. Hence, it is impossible to predict the true extent of this supernova remnant based on the structure of the visible shell segement alone.

I performed a flux integration over the area of the visible shell segment as seen in Fig. 1 (lower panels) and Fig. 2 only. The shell segment has integrated flux densities of 65 ± 7 mJy at 1420 MHz and 140 ± 15 mJy at 408 MHz. This implies a spectral index of $\alpha = -0.6 \pm 0.1$ ($S \sim \nu^{\alpha}$). The integrated polarized intensity is 32 ± 4 mJy which gives an unprecedented 50% integrated polarization at 1420 MHz. At the peak of the polarized intensity the percentage polarization increases to about 71% which is the theoretical maximum for a synchrotron spectrum with a spectral index of $\alpha = -0.6$ and implies that there is no depolarization. To achieve such a high percentage polarization a tangential magnetic field structure within the shell is required. The swept up material must be completely dominating the hydrodynamics of the remnant and the characteristics of the synchrotron emission. This implies a highly evolved SNR, at least within the shell segment.

Table 1. Polarization angles calculated for the 4 bands of the CGPS at the two peaks in polarized intensity. The intrinsic polarization angle, measured for a tangential magnetic field, is indicated at 0 cm.

Band	Wavelength	Pixel 1	Pixel 2
A	21.324 cm	$-4 \pm 4°$	$22 \pm 4°$
B	21.219 cm	$-1 \pm 5°$	$15 \pm 5°$
C	21.017 cm	$-2 \pm 5°$	$21 \pm 5°$
D	20.916 cm	$-3 \pm 5°$	$18 \pm 5°$
	0 cm	$56 \pm 5°$	$70 \pm 5°$

3.2. Rotation measures

The CGPS polarization data consists of 4 bands around 21 cm, and I attempted to calculate rotation measures (*RM*) for the polarized shell. Unfortunately the signal-to-noise ratio in the individual bands is rather low for most parts of the structure and I was able to calculate *RM*s only for two peaks in polarized intensity at $l_1 = 107.27°$, $b_1 = -1.70°$ and at $l_2 = 107.24°$, $b_2 = -1.65°$. For both peaks the measured polarization angles in the four bands are equal within the errors, yielding *RM*s close to 0 with errors of about ± 55 rad/m^2 (see Table 1). Fortunately we know that the magnetic field structure must be tangential to the shell and the intrinsic polarization angles must be perpendicular to it. Using this information I fitted the rotation measure again, finding $RM_1 = -23 \pm 2$ rad/m^2 and $RM_2 = -20 \pm 2$ rad/m^2 (see Fig. 3). Since at 1420 MHz the polarization angle could have been rotated by $\pm\pi$ I have to discuss the possibility of higher rotation measures. The latest studies of rotation measures for extra galactic sources (Brown et al. 2003, and Jo-Anne Brown, private communication) as well as for pulsars (Mitra et al. 2003) agree that the magnetic field in this direction of the Galaxy is directed away from us. In this case we can neglect the possibility of a positive rotation measure. The next feasible negative *RM* would be about -93 rad/m^2. This would lead to a difference in polarization angle of $10°$ between Band *A* and Band *D* exceeding the errors by a factor of 2. Thus I can discard the possibility of higher rotation measures.

3.3. The environment

The appearance of a supernova remnant strongly depends on the structure of the ambient medium. Hence to explain the peculiar shape of the remnant I examined images of H I and CO from the CGPS database (the CO observations are from the Five College Radio Astronomy Observatory by Heyer et al. 1998). An inspection of the area around G107.5−1.5 did not reveal any possibly correlated molecular material.

In the H I maps, however, multiple structures at almost all allowed radial velocities are visible. Naively one would expect an H I enhancement just outside the radio shell. Indeed at a velocity of about -50 km s^{-1} such a structure is present (Fig. 4). Additionally away from the radio shell there is a gap in the H I emission indicating that there the shock wave is still expanding freely. This looks like a perfect match, but a radial velocity of -50 km s^{-1} would suggest a location within the Perseus arm. Such a large distance is ruled out by the high

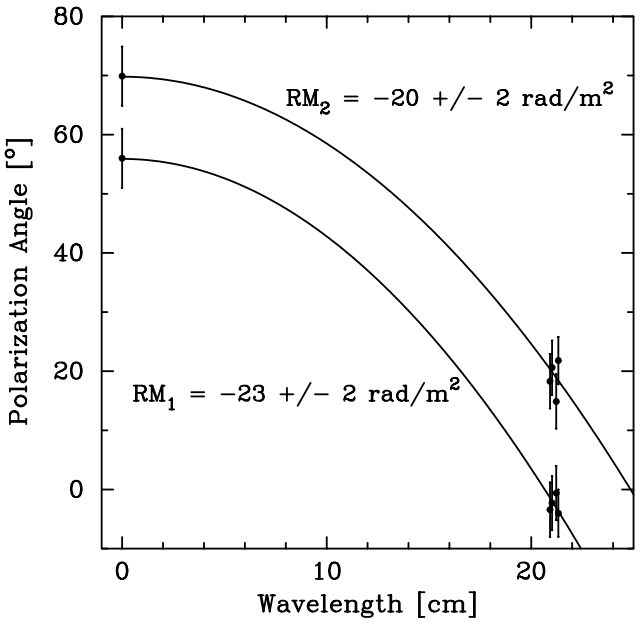

Fig. 3. Diagram of the polarization angle as a function of wavelength for the two peaks in polarized intensity. The fitted functions for the rotation measure are indicated.

percentage polarization and the low rotation measure. At local radial velocities no such structure is visible, but at a radial velocity of about -9 km s^{-1} the exact opposite circumstances are present (Fig. 4). At the position of the radio shell there is a depression in the H I emission. We could argue that the supernova shock wave expanded into very dense material outside the visible radio shell and decelerated very quickly, while the part at the position of the radio shell expanded into moderately dense material and is still energetic enough to generate detectable radio emission. Since the polarization provides a very strong argument for a short distance I take the structure at -9 km s^{-1} to be the more likely environment around the new SNR, but this coincidence cannot be taken as a definite indicator of the distance to the SNR.

Another point for the environment at the shorter distance is that we require a highly evolved remnant to explain the high percentage polarization. The ambient medium structure at the shorter distance implies that the other parts of the remnant are even further evolved than the visible shell, which is a reasonable explanation why they are not observable anymore. On the other hand the ambient medium structure at -50 km s^{-1} suggests that the other parts of the remnant are less evolved than the visible shell. To be not observable those parts have to be very young and we would expect that the radio emission would increase from the visible filament towards the HI gaps before it drops because a supernova remnant is supposed to be brightest at the beginning of the Sedov phase when the interaction between the ejecta and the swept up material is strongest. Since this is not the case here the shorter distance is much more likely.

4. Discussion

With an integrated fractional polarization of about 50% and peak polarization of up to 70%, G107.5−1.5 is the most highly polarized shell-type supernova remnant known. A highly homogeneous magnetic field is necessary to create such a high percentage polarization. The theoretical maximum for a synchrotron spectrum with $\alpha = -0.6$ is 71%. This requires a well evolved supernova remnant in which the swept-up material with its frozen-in tangential magnetic field dominates the hydrodynamics. Young SNRs with their radial magnetic field have a much smaller fractional polarization due to turbulence created by the interaction of the ejecta with the ambient medium. Observed percentage polarization for these sources is usually below 10% (see Anderson et al. 1995; Kothes & Reich 2001; DeLaney et al. 2002; Reynolds & Gilmore 1993; Dickel et al. 1991, for Cas A, G11.2−0.3, Kepler, SN 1006, and Tycho, respectively). However, older shell-type SNRs are known to have very high fractional polarization. The record is currently held by G182.4+4.3 with also about 50% integrated polarization and peaks of over 60% at 6 cm wavelength (Kothes et al. 1998). Given the fact that radio emission at longer wavelength suffers more from depolarization, this extremely high percentage polarization of G107.5−1.5 at 1420 MHz is even more remarkable.

4.1. The ROSAT point source 1RXS J225203.8+574249

Close to the projected centre of the radio shell there is an unidentified, faint X-ray point source, listed in Voges et al. (2000) as 1RXS J225203.8+574249 with a total of 13 counts in the ROSAT All-sky survey. Unfortunately we cannot draw any conclusions about its nature since 13 counts are hardly enough to deduce any spectral information. However, the position of this source is quite compelling (see Fig. 1). It is not only close to the projected centre of the shell, if it is a neutron star and the explosion happened at its current position it would explain the peculiar appearance of the SNR quite nicely. In all directions the wind of the progenitor and the shock wave of the explosion would have been blocked by dense neutral hydrogen except for the gap in the direction of the radio shell. Due to its position at $l = 107.5°$ and $b = -1.5°$ which approximately coincides with the projected centre of the radio shell (see Fig. 1), I have named this new SNR G107.5−1.5.

4.2. The distance

The low *RM* values point to a rather short distance placing G107.5−1.5 within the local arm. To quantify this statement I investigated the magnetic field structure and electron distribution in this direction. Mitra et al. (2003) found the foreground magnetic field parallel to the line of sight $B_{\|}$ for pulsars in this region (in their paper region 2) to be about -1 μGs calculated for pulsars which are supposed to be in areas free from foreground H II regions. The rotation measure is defined as:

$$RM = 0.812 \cdot B_{\|} \cdot DM, \quad (1)$$

where *DM* is the dispersion measure in units of pc cm^{-3}. For a mean foreground rotation measure of -21.5 rad/m^2 and $B_{\|} = -1$ μGs I find a foreground dispersion measure of

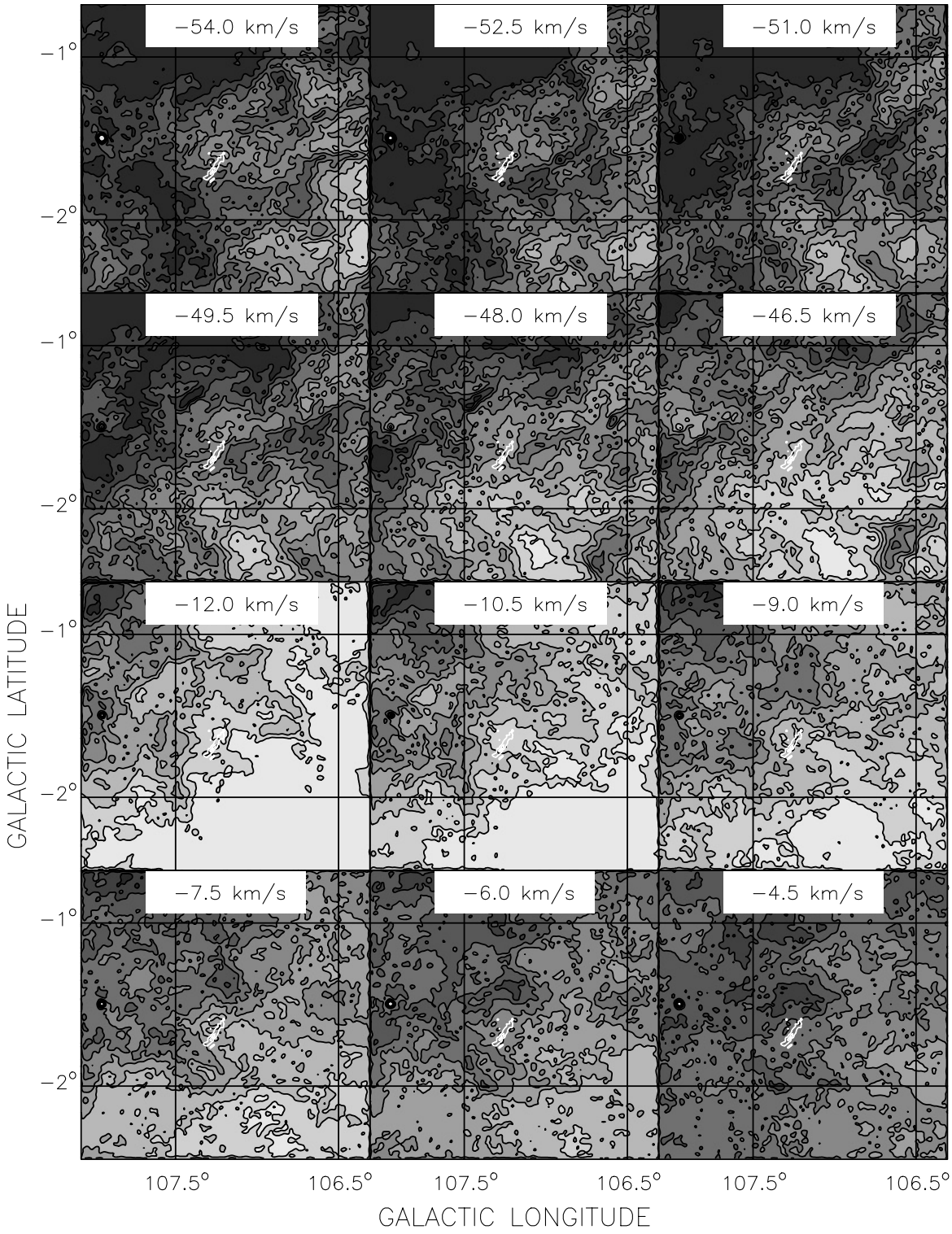

Fig. 4. H I channel maps taken from the CGPS data centered on the new SNR G107.5−1.5. Black contours are at 25, 32, 39, 46, 53, 60, 67, and 74 K T_B. White contours indicate the radio continuum emission at 1420 MHz.

DM = 26.5 pc cm^{-3}. The models of free electrons in our Galaxy by Taylor & Cordes (1993) and Cordes & Lazio (2003) give 1.4 kpc and 1.6 kpc for this dispersion measure respectively. Since we do not know how much of the rotation measure arises from internal effects and how much from the foreground, these distances are upper limits. The three pulsars used to determine the foreground magnetic field listed in Mitra et al. (2003) are Perseus arm objects, thus this mean foreground magnetic field contains the interarm. Since G107.5−1.5 is located within the local arm the foreground magnetic field should be higher, which is another indication that the determined distance is an upper limit.

With a radial velocity of −9 km s^{-1} for the H I structures around G107.5−1.5 we can estimate a kinematic distance.

A flat rotation curve for the Galaxy with $R_\odot = 8.5$ kpc and $v_\odot = 220$ km s^{-1} gives a distance of about 1.1 kpc.

I also used the new distance estimation method from Foster & Routledge (2003) to determine a third value. The method constructs models that trace the radial distribution of Galactic H I. These models depend on the location in the plane (ℓ, b), the distance to the Galactic warp, the scale length and scale height of the H I disk, and the distribution of H I through the spiral arms encountered along the line of sight. The profile is calibrated by calculating the neutral hydrogen column density to the Galactic edge $N_{\rm HI}(r = \infty)$. The hydrogen column density in the foreground of the object is then used to locate the distance to the object on the calculated H I distribution. I averaged the H I emission over the proposed area of the SNR to determine an H I profile as a function of radial velocity. By assuming that the radial velocity is decreasing with distance, I integrated the foreground H I emission of the SNR. The results were $N_{\rm HI}^{\rm edge} = 5.8 \times 10^{21}$ cm^{-2} and $N_{\rm HI}^{\rm SNR} = 1.4 \times 10^{21}$ cm^{-2} for an assumed radial velocity of -9 km s^{-1}. This results in a distance of 0.7 ± 0.3 kpc.

Averaging all determined distances gives $d = 1.1 \pm 0.4$ kpc for the new supernova remnant. The length of the filament of 12′ translates to 4 pc and the 18′ distance from 1RXS J225203.8+574249 to a radius of 6 pc. With a diameter of 36′ and an interpolated flux density of about 80 mJy at 1 GHz this SNR would have a radio surface brightness of $\Sigma_{1\ \rm GHz} = 10^{-23}$ Watt m^{-2} Hz^{-1} sr^{-1} which is a factor of about 6 smaller than the brightness of G156.2+5.7 (Reich et al. 1992), which is the lowest currently listed in Green's catalogue of Galactic supernova remnants (Green 2001). However, this radio surface brightness is a lower limit, because the diameter was interpolated from the radius of the visible shell, which is the youngest part of the SNR. The radius of the invisible parts, by being older, should be significantly smaller. But the SNR is still a very faint radio source.

The high fractional polarization, the ambient medium structure, and the low radio surface brightness point to a supernova remnant in a rather late stage of evolution.

Assuming the SNR has just entered the so-called radiative pressure-driven snowplow phase as defined by Cioffi et al. (1988), we derive a mean ambient density for the visible radio shell of about 1 to 7 cm^{-3} for explosion energies between 10^{50} and 10^{51} erg. This will lead to an age between about 3000 and 6000 yrs for G107.5−1.5. Given the fact that the SNR either had a low explosion energy or a rather high ambient medium density, the low age and small radius are not that unsusual for a far developed SNR.

5. Summary

The new supernova remnant G107.5−1.5 has been discovered with data from the Canadian Galactic Plane Survey through its highly polarized radio emission and a spectral index of $\alpha = -0.6 \pm 0.1$ indicative of a shell-type SNR. This remnant is located in the local spiral arm at a distance of about 1.1 kpc, which gives it a radius of about 6 pc. At its projected centre there is the unidentified X-ray source 1RXS J225203.8+574249, which could indicate a neutron star or a pulsar wind nebula, objects we expect to find in an SNR in a complex environment like G107.5−1.5. No molecular material has been found in the ambient medium, but a depression in the H I distribution coinciding with the radio bright shell segment could indicate that it is expanding in a moderate dense ambient medium while the other parts of the SNR expanded into a very dense environment, decelerated very quickly and do not show any detectable emission anymore.

Acknowledgements. I wish to thank Tyler Foster for providing a distance to G107.5−1.5 with his new method. I also like to thank Tom Landecker for careful reading of the manuscript. The Dominion Radio Astrophysical Observatory is a National Facility operated by the National Research Council. The Canadian Galactic Plane Survey is a Canadian project with international partners, and is supported by the Natural Sciences and Engineering Research Council (NSERC).

References

Anderson, M. C., Keohane, J. W., & Rudnik, L. 1995, ApJ, 441, 300
van den Bergh, S., & McClure, R. D. 1994, ApJ, 425, 205
Brown, J. C., Taylor, A. R., & Jackel, B. J. 2003, ApJ, 145, 213
Cordes, J. M., & Lazio, T. J. 2003 [astro-ph/0207156]
Cioffi, D. F., McKee, C. F., & Bertschinger, E. 1988, ApJ, 334, 252
DeLaney, T., Koralesky, B., Rudnik, L., & Dickel, J. R. 2002, ApJ, 580, 914
Dickel, J. R., van Breugel, W. J. M., & Strom, R. G. 1991, AJ, 101, 2151
Foster, T., & Routledge, D. 2003, ApJ, submitted
Green, D. A. 2001, A Catalogue of Galactic Supernova Remnants (2001 December version), Mullard Radio Astronomy Observatory, Cavendish Laboratory, Cambridge, UK (available on the World-Wide-Web at http://www.mrao.cam.ac.uk/surveys/snrs/)
Haslam, C. G. T., Stoffel, H., Salter, C. J., & Wilson, W. E. 1982, A&AS, 47, 1
Heyer, M. H., Brunt, C., Snell, R. L., et al. 1998, ApJS, 115, 241
Higgs, L. A., & Tapping, K. F. 2000, AJ, 120, 2471
Kothes, R., Fürst, E., & Reich, W. 1998, A&A, 331, 661
Kothes, R., & Reich, W. 2001, A&A, 372, 627
Kothes, R., Landecker, T. L., Foster, T., & Leahy, D. A. 2001, A&A, 376, 641
Kothes, R., Uyaniker, B., & Yar, A. 2002, ApJ, 576, 169
Landecker, T. L., Dewdney, P. E., Burgess, T. A., et al. 2000, A&AS, 145, 509
Mitra, D., Wielebinski, R., Kramer, M., & Jessner, A. 2003, A&A, 398, 993
Reich, W., Fürst, E., & Arnal, E. M. 1992, A&A, 256, 214
Reich, W., Reich, P., & Fürst, E. 1990, A&AS, 83, 539
Reynolds, S. P., & Gilmore, D. M. 1993, AJ, 106, 272
Taylor, J. H., & Cordes, J. M. 1993, ApJ, 411, 674
Taylor, A. R., Gibson, S. J., Peracaula, M., et al. 2003, AJ, 125, 3145
Voges, W., Aschenbach, B., Boller, T., et al. 2000, IAU Circ., 7432, 1